esa ECOSPHERE

Ecosystem warming increases sap flow rates of northern red oak trees

Stephanie M. Juice,[1] Pamela H. Templer,[1,†] Nathan G. Phillips,[2] Aaron M. Ellison,[3] and Shannon L. Pelini[4]

[1]*Department of Biology, Boston University, Boston, Massachusetts 02215 USA*
[2]*Department of Earth and Environment, Boston University, Boston, Massachusetts 02215 USA*
[3]*Harvard University, Harvard Forest, Petersham, Massachusetts 01366 USA*
[4]*Department of Biological Sciences, Bowling Green State University, Bowling Green, Ohio 43403 USA*

Citation: Juice, S. M., P. H. Templer, N. G. Phillips, A. M. Ellison, and S. L. Pelini. 2016. Ecosystem warming increases sap flow rates of northern red oak trees. Ecosphere 7(3):e01221. 10.1002/ecs2.1221

Abstract. Over the next century, air temperature increases up to 5°C are projected for the northeastern United States. As evapotranspiration strongly influences water loss from terrestrial ecosystems, the ecophysiological response of trees to warming will have important consequences for forest water budgets. We measured growing season sap flow rates in mature northern red oak (*Quercus rubra* L.) trees in a combined air (up to 5.5°C above ambient) and soil (up to 1.85°C above ambient at 6-cm depth) warming experiment at Harvard Forest, Massachusetts, United States. Through principal components analysis, we found air and soil temperatures explained the largest amount of variance in environmental variables associated with rates of sap flow, with relative humidity, photosynthetically active radiation and vapor pressure deficit having significant, but smaller, effects. On average, each 1°C increase in temperature increased sap flow rates by approximately 1100 kg H_2O m^{-2} sapwood area day^{-1} throughout the growing season and by 1200 kg H_2O m^{-2} sapwood area day^{-1} during the early growing season. Reductions in the number of cold winter days correlated positively with increased sap flow during the early growing season (a decrease in 100 heating-degree days was associated with a sapflow increase in approximately 5 kg H_2O m^{-2} sapwood area day^{-1}). Soil moisture declined with increased treatment temperatures, and each soil moisture percentage decrease resulted in a decrease in sap flow of approximately 360 kg H_2O m^{-2} sapwood area day^{-1}. At night, soil moisture correlated positively with sap flow. These results demonstrate that warmer air and soil temperatures in winter and throughout the growing season lead to increased sap flow rates, which could affect forest water budgets throughout the year.

Key words: climate change; mixed temperate forest; *Quercus rubra*; transpiration; warming experiment; water uptake.

Received 23 July 2015; accepted 28 July 2015. Corresponding Editor: D. P. C. Peters.

Copyright: © 2016 Juice et al. This is an open access article under the terms of the Creative Commons Attribution License, which permits use, distribution and reproduction in any medium, provided the original work is properly cited.

† **E-mail:** ptempler@bu.edu

Introduction

In the northeastern United States, air temperatures have increased 0.25°C per decade since 1970 (Hayhoe et al. 2007) and warming is projected to continue over the next century with a cumulative increase between 2.5 and 5.6°C by 2100 (Horton et al. 2014). Projections of rising air temperature in this region are accompanied by forecasts of increased occurrence of seasonal drought and extended periods of low stream flow during the growing season (Hayhoe et al. 2007). Indeed, changing temperatures worldwide are projected to alter water dynamics on land, with the balance between precipitation and potential evapotranspiration (PET) determining

the aridity of a location (Feng and Fu 2013). PET is the rate of evapotranspiration (ET) that would be observed if water were not limited, and can be thought of as the "price" a plant pays to keep its stomata open (Scheff and Frierson 2014). As plant activity strongly affects the movement of water through terrestrial ecosystems, transpiration dominates evaporative loss over land, and transpiration itself accounts for 80–90% of terrestrial ET (Jasechko et al. 2013). The strong biological control over terrestrial ET necessitates better estimates of the effects of increased temperatures on water uptake by trees to project future forest water balances.

Measurement of xylem sap flow via thermal dissipation probes is a widely used method for estimation of whole-tree transpiration (Swanson 1994, Granier et al. 1996a, Lu et al. 2004). Observational studies have found that rates of sap flow are positively correlated with ambient air temperature (PengSen et al. 2000, Juhász et al. 2013, Chang et al. 2014). However, other studies have shown stronger relationships between sap flow rates and vapor pressure deficit (VPD) compared to air temperature (Yin et al. 2004). A warming experiment with young (~30 yr old) *Picea abies* (L.) H. Karst. trees in Sweden showed that warmer soils led to greater rates of sap flow, but measurements of sap flow were limited to the beginning of the growing season and differences were apparent only when snow covered reference plots (Bergh and Linder 1999). Another study examining the effects of experimental warming on rates of sap flow in young *Pinus engelmannii* Carr. trees found no effect of experimental warming on rates of sap flow, but measurements were limited to the snowmelt period (Day et al. 1990). We are not aware of any studies examining the effects of experimental ecosystem warming on rates of sap flow throughout the growing season by mature trees in a temperate deciduous forest. Changes in sap flow rates caused by increased temperatures or changes in VPD could have cascading effects on forest water balance and stream flow in forest ecosystems. For example, because black birch (*Betula lenta* L.) has higher rates of sap flow than eastern hemlock (*Tsuga canadensis* (L.) Carr.), the water budget of a temperate forest in central Massachusetts (United States) was altered as hemlock trees were killed by hemlock woolly adelgid (*Adelges tsugae* Annand) and replaced by black birch (*B. lenta* L.). The hydrological flow of adjacent streams was much lower in summer following loss of hemlock (Daley et al. 2007), a finding that has been replicated elsewhere (Ford and Vose 2007).

Here, we describe the results of a novel study examining effects of both warmer air and soil temperatures on the rate of sap flow in mature northern red oak (*Quercus rubra* L.) trees throughout the growing season. We took advantage of an open-top chamber warming experiment at Harvard Forest to test the hypothesis that warmer air and surface soil temperatures lead to greater rates of sap flow by red oak trees. We examined the response of sap flow rates to experimental warming in the early growing season (24-h rates), throughout the growing season (24-h rates) and at night when photosynthetically active radiation (PAR) was less than zero (typically between 2200 and 0500 h). We expected rates of sap flow to increase in response to experimental warming because observational studies have shown a positive relationship between ambient air temperatures and rates of sap flow (Bergh and Linder 1999, PengSen et al. 2000, Juhász et al. 2013, Chang et al. 2014). We also expected night time sap flow to increase in response to warmer soils, as night time transpiration has been documented in trees at Harvard Forest (Daley and Phillips 2006, Phillips et al. 2010). We expected early growing season rates of sap flow to respond positively to warmer soil temperatures in winter due to reductions in soil freezing, which has been shown to damage roots (Tierney et al. 2001, Comerford et al. 2013). We also predicted that warmer temperatures induced by experimental treatments would lead to changes in soil moisture that could affect rates of sap flow. Any observed changes in rates of sap flow by red oak trees could have cascading effects on forest water dynamics and canopy carbon exchange in this forest.

Methods

Study site

This research was conducted in the Prospect Hill Tract of Harvard Forest. Mean annual air temperature for Harvard Forest is 7.1°C, and mean annual precipitation is 1066 mm (Boose 2001). Soils are predominately coarse loam acidic

Table 1. Experimental chamber properties including mean increase in temperature ($\Delta T_{chamber}$, in °C) over ambient for air and soil at two depths, targeted increase in air temperature ($\Delta T_{chamber}$, in °C), volumetric water content (VWC) of the upper 15 cm of soil during the period of sap flow measurements, and diameter at breast height (DBH, in centimeters) of each red oak tree. $\Delta T_{chamber}$ values are means with standard error, zeros indicate controls.

Mean air $\Delta T_{chamber}$	Mean soil $\Delta T_{chamber}$ at 2 cm	Mean soil $\Delta T_{chamber}$ at 6 cm	Target air $\Delta T_{chamber}$	VWC	DBH	Chamber
0	0	0	0	0.116	20.3	4
0	0	0	0	0.167	26.4	6
0	0	0	0	0.165	46.0	11
1.76 ± 0.34	0.40 ± 0.19	0.27 ± 0.22	2.5	0.186	49.8	9
1.81 ± 0.17	0.56 ± 0.08	0.90 ± 0.20	1.5	0.124	41.1	8
2.09 ± 0.10	0.39 ± 0.20	0.45 ± 0.21	2.0	0.117	39.4	3
2.75 ± 0.44	0.78 ± 0.29	0.84 ± 0.14	3.5	0.203	37.6	12
3.29 ± 0.22	1.26 ± 0.34	0.91 ± 0.33	3.0	0.116	50.8	7
4.03 ± 0.31	1.13 ± 0.25	0.98 ± 0.21	4.5	0.203	41.7	10
4.49 ± 0.31	1.58 ± 0.22	1.73 ± 0.16	4.0	0.130	22.9	2
4.95 ± 0.25	2.13 ± 0.15	1.85 ± 0.28	5.0	0.129	29.5	5
5.23 ± 0.34	1.65 ± 0.45	1.78 ± 0.76	5.5	0.131	47.0	1

Gloucester series dystrochrepts derived from glacial till (McFarlane et al. 2013). Overstory vegetation is classified as a transition hardwood forest (Foster and Aber 2004) and is dominated by oaks (*Quercus* spp.), red maple (*Acer rubrum* L.), birches (*Betula* spp.), white ash (*Fraxinus americana* L.), and American beech (*Fagus grandifolia* Ehrh.); dominant conifer species include eastern hemlock (*T. canadensis*) and white pine (*Pinus strobus* L) (Foster 1992).

Experimental design

Our study was conducted within an ongoing warming experiment. The design of the experiment is described thoroughly by Pelini et al. (2011); only salient details are presented here. Twelve open-top octagonal chambers (5-m diameter, 1.2-m tall; internal volume = 21.7 m^3) were installed in 2009 in a forest tract dominated by ~70-yr-old northern red oak and red maple trees. Each chamber is centered around an overstory northern red oak tree; the diameters (measured at 1.3 m aboveground) of the 12 trees used in this study ranged from 20 to 50 cm. Forced air was blown in to each chamber through 15 cm diameter plastic plena 45 cm above the ground in two concentric circles per chamber. Open-top chambers with warm air blown in minimizes soil disturbance compared to other warming methods used in forest ecosystems, such as soil cables (Pelini et al. 2011). Air blown into the open-top chamber was unlikely to reach the upper canopy of the overstory northern red oak trees and therefore the warming treatment was similar to other ecosystem warming experiments in forest ecosystems, where enhanced temperature treatments were constrained to the soil and in this case the lower parts of the tree. Although wind has been shown to affect rates of sap flow (Yin et al. 2004), it was unlikely to be a confounding factor in this study since the chambers were randomly distributed and all of the red oaks were within a single stand of trees.

Between January 2010 and July 2015, the three control chambers received continuously unheated forced air, whereas the treatment chambers were continuously heated with air blown over hot-water radiators. Set points for increases in temperature over ambient air temperature in the nine treatment chambers (hereafter referred to as "$\Delta T_{chamber}$") ranged from 0.5°C to 5.5°C (Table 1). In this regression design (Cottingham et al. 2005), the continuous range of $\Delta T_{chamber}$ can reveal nonlinearities or threshold responses of ecosystem processes to changes in temperature (Pelini et al. 2011). In each chamber, air temperature (n = 2 sensors per chamber), soil temperature at 2-cm depth (n = 2 sensors per chamber), and soil temperature at 6-cm depth (n = 2 sensors

per chamber) were all measured with Betatherm-type 10K3A1 thermistors (Campbell Scientific, Logan, Utah, USA). Actual $\Delta T_{chamber}$ values of air and soil temperatures in each chamber were calculated by first averaging the data from the three control chambers, and then subtracting that average from each of the nine treatment chamber's temperatures to obtain one $\Delta T_{chamber}$ value per treatment chamber over time. In addition, PAR (n = 1 sensor per chamber, model SQ110; Apogee Instruments Inc., Logan, Utah, USA), relative humidity (RH; n = 1 sensor per chamber, HS-2000V capacitive polymer sensors; Precon, Memphis, Tennessee, USA), and soil volumetric water content (VWC) from 0 to 15 cm depth (n = 1 sensor per chamber; model CS616; Campbell Scientific) were measured. All measurements occurred at 1-min intervals and hourly means were saved to a CR1000 data logger (Campbell Scientific). Chamber-level VPD was calculated using the air temperature and RH from each chamber.

In addition to the measurements taken within each chamber, RH and air temperature outside the chambers were measured using a Campbell Scientific HMP45C installed at 2-m height in a non-heated location in the center of the group of chambers. Air temperature and RH at this location was measured every 30 s using a CR1000 data logger; half-hour averages were used to calculate canopy-level VPD, which was used as a guide for determination of sap flow.

Sap flow measurements

Sap flux density measurements were made using thermal dissipation probes consisting of a pair of 1-mm diameter, 11 mm long stainless-steel hollow needles with copper constantan (type T) thermocouples inserted at the midpoint (Granier 1987). As the majority of sap flow in oak trees occurs in the outermost growth rings ("sap wood"; Granier et al. 1994), a sensor length of 11 mm captures the flow in these rings while avoiding an underestimation of sap flow due to radial gradients inherent to ring-porous trees such as red oak (Phillips et al. 1996, Clearwater et al. 1999, James et al. 2002). One probe in each pair (hereafter referred to as the "heated probe") was wound with electrically insulated constantan heating wire, which received 185 mW of constant power. The other probe was left unheated.

Probes were installed in April 2011 in freshly drilled holes at 1.3-m height on both the north and south side of the trunk of each of the 12 trees. A vertical distance of 10 cm separated the lower unheated probe from the upper heated probe. Heated probes were first coated with heat-conducting silicon paste and inserted into aluminum tubes that were pre-installed in the sap wood. The constantan leads from the two probes were joined, so that the differential voltage measured across the copper leads represented the temperature difference (ΔT_{sap}) between the two thermocouples. The ΔT_{sap} therefore varies inversely with rates of sap flow in the tree, which dissipates the heat supplied to the downstream sensor. Sensors were sealed under plastic containers with acid-free silicone caulk to protect them from precipitation, and then covered with reflective bubble wrap to prevent heating caused by direct solar radiation. Differential voltages within each of the sensors were measured every 30 s and averaged every half-hour to ensure a fine scale resolution of temporal sap flow gradients (Clearwater et al. 1999). Data were recorded using AM16/32B multiplexers and stored in a CR1000 multichannel data logger.

Data analysis and statistics

Sap flow per unit conducting xylem area (J_S, in g H_2O m^{-2} sapwood area s^{-1}) was calculated by first determining the zero sap flow condition in the tree ($\Delta T_{sap\ max}$, between upper and lower probes within each tree). Environmental factors that affect stem water content cause variation in $\Delta T_{sap\ max}$ over time (Lu et al. 2004), necessitating frequent re-definition of the zero-flow state. For periods not longer than 10 d, $\Delta T_{sap\ max}$ was determined to have occurred when the following two conditions were met: (1) the temperature gradient between the reference and heated probes was stable for at least 2 h; and (2) the ambient VPD was calculated to be <0.1 kPa. Determining $\Delta T_{sap\ max}$ according to these two conditions allowed for nighttime sap flow to be calculated directly rather than assuming night time zero-flow condition, which can underestimate total sap flow (Lu et al. 2004, Oishi et al. 2008). After $\Delta T_{sap\ max}$ was determined, sap flow rates were calculated using the empirical relationship between sap velocity and the rate of sap flow described by Granier (1987):

$$J_S = 119\left(\frac{\Delta T_{sapmax} - \Delta T_{sap}}{\Delta T_{sap}}\right)^{1231} \quad (1)$$

where ΔT_{sap} (°C) is the temperature difference between the heated and unheated sensors at any given time. All conversions from differential voltages to sap flow were done using BaseLiner software (version 3.0.10, developed by Ram Oren, Duke University).

Sap flow was measured continuously throughout the growing season, but we used only 15 d of data for which we had 24 h of both continuous sap flow data and environmental variables; on other days, gaps in the data were caused by power outages or loss of data when cables were chewed by animals. These 15 d – days of year (DOY) 126–127, 131–132, 178, 229–232, 235–236, and 294–297 – spanned the growing season. The 15 d also each had relatively high VPD and thus excluded days of suppressed sap flow rates (sap flow is highly correlated with VPD; Granier et al. 1996b).

The daily sum of sap flow was calculated for each sensor for each of the 15 d of the study. The driving influence of environmental variables on sap flow was then analyzed according to three different periods. First, daily sums of sap flow for all 15 measurement days were analyzed for the effect of warming on sap flow rates for the entire study period. Next, nighttime sap flow (when PAR in the chambers measured ≤0, normally between the hours of 2200–0500) was analyzed to examine potential effects of warmer nights on sap flow rates. Last, sap flow from the first four measurement days (DOY 126, 127, 131, and 132) was regressed against winter environmental conditions to examine the effects of winter warming on early growing season sap flow dynamics. For this last analysis, heating degree days (HDD) for each chamber were calculated for the three winter months (December 1, 2010 until February 28, 2011) as the difference between the observed daily mean temperature and 18°C. High HDD's correspond to relatively colder temperatures, whereas low HDDs correspond to relatively warmer temperatures. For each sap flow period (24-h, nighttime, and early growing season sap flow), we examined potential relationships between rates of sap flow and measured environmental variables (maximum, mean, and minimum air temperature and soil temperature at 2- and 6-cm depths, and PAR, RH, VPD, and VWC). HDD was included as an environmental variable only for the early growing season analysis. As many of these variables are correlated with one another, we used principal components analysis (PCA) to create composite environmental scores from all of these environmental variables. Regressions of sap flow measurements on PC scores then illustrate dependencies of sap flow on overall environmental conditions.

All statistical analyses were done using various functions within the R statistical software system, version 3.0.3 (R Core Team 2013). All raw data and R code used to analyze the data are available from the Harvard Forest Data Archive (http://harvardforest.fas.harvard.edu/data-archive), dataset HF247.

Results

The experimental infrastructure successfully elevated air temperatures and raised soil temperatures at both 2 and 6 cm soil depth (Table 1). There was a significant positive correlation (r = 0.60, P < 0.0001) between sap flow rates measured on the north and south side of the individual trees. However, sap flow responded differently to environmental variables depending on the side of the tree on which it was measured (north vs. south) and so sensor location was included as a covariate in all analyses. VWC varied among the chambers (Table 1), declining with increased treatment temperatures (slope = −0.005, R^2 = 0.19, P < 0.0001 for soil temperatures measured at both 2- and 6-cm depths). Nearly all the environmental variables were correlated with each other to some degree (Table 2). Some of the strongest correlations were between air and soil temperature, PAR and RH, and RH and VPD. These patterns were reflected in their loadings in the PCA (Tables 3 and 4).

Through PCA, we found air and soil temperatures explained the largest amount of variance in environmental variables associated with rates of sap flow throughout the growing season, with RH, PAR, and VPD having significant, but smaller effects on sap flow (Figs. 1 and 2). On average, each 1°C increase in temperature increased sap flow rates by approximately 1100 kg H_2O m^{-2}

Table 2. Pearson correlation coefficients (*r* values) between environmental variables.

	Soil temp (2 cm)	Soil temp (6 cm)	PAR	RH	VWC	VPD
Air temp	0.89	0.79	0.13	0.02	0.36	0.63
Soil temp (2 cm)		0.97	0.47	0.32	0.44	0.32
Soil temp (6 cm)			0.58	0.38	0.46	0.22
PAR				0.60	0.08	0.39
RH					0.01	0.73
VWC						0.21

Note: PAR, photosynthetically active radiation; RH, relative humidity; VPD, vapor pressure deficit; VWC, volumetric water content.

Table 3. Environmental variable loadings on the first three principal axes for analysis of 24-h sap flow.

Variable	Axis 1 "temperature"	Axis 2 "RH, PAR, VPD"	Axis 3 "soil moisture"
Air temperature	**−0.2595**	0.2008	−0.1783
Min air temperature	**−0.2660**	0.1853	−0.1689
Max air temperature	**−0.2519**	0.2161	−0.1876
Soil temperature (2 cm)	**−0.3087**	0.0503	−0.0805
Min soil temperature (2 cm)	**−0.3091**	0.0459	−0.0806
Max soil temperature (2 cm)	**−0.3080**	0.0550	−0.0804
Soil temperature (6 cm)	**−0.3091**	−0.0022	−0.0382
Min soil temperature (6 cm)	**−0.3093**	−0.0052	−0.0387
Max soil temperature (6 cm)	**−0.3089**	0.0012	−0.0377
RH	−0.1311	**−0.3646**	0.0420
Min RH	−0.1306	**−0.3681**	0.0443
Max RH	−0.1297	**−0.3586**	0.0380
PAR	0.1806	**0.2928**	0.0220
Min PAR	0.2049	**0.2547**	0.0403
Max PAR	0.1403	**0.3191**	−0.0054
VWC	0.1622	−0.1373	**−0.5396**
Min VWC	0.1609	−0.1390	**−0.5220**
Max VWC	0.1553	−0.1285	**−0.5330**
VPD	−0.0663	**0.4084**	−0.1599

Notes: PAR, photosynthetically active radiation; RH, relative humidity; VPD, vapor pressure deficit; VWC, volumetric water content.Values >0.25 (bold) were considered "heavily loading" on the axis.

sapwood area day^{-1} throughout the growing season and by 1200 kg H_2O m^{-2} sapwood area day^{-1} during the early growing season. Reductions in the number of cold winter days correlated positively with increased sap flow during the early growing season (a decrease of 100 heating-degree days was associated with a sapflow increase of approximately 5 kg H_2O m^{-2} sapwood area day^{-1}).

The first three principal axes of the PCA cumulatively explained 91.3% and 87.4% of the variance in environmental variables associated with daily (24-h) and nighttime sap flow, respectively, across the 15 measurement days (Tables 3 and 4; Figs. 1–4). The first axis (referred to as "*temperature*") explained 53.3% and 49.9% of the variance in environmental variables associated with the daily and nighttime data, respectively, and was correlated negatively with all metrics (average, maximum, minimum) of air and soil temperatures for the daily data, but correlated positively with the nighttime data. The second axis ("*RH, PAR, VPD*") explained an additional 26.5% of the variance in the environmental variables for the daily data, and was positively correlated with metrics of PAR and VPD, and negatively correlated with metrics of RH. In contrast, the second axis for the nighttime data ("*RH, VPD*") was positively correlated with VPD and negatively correlated with metrics of RH, and it explained an additional 20.9% of the variance in the data. The third axis ("*soil moisture*") was negatively correlated

Table 4. Environmental variable loadings on the first three principal axes for analysis of nighttime sap flow.

Variable	Axis 1 "Temperature"	Axis 2 "RH, VPD"	Axis 3 "PAR, Soil Moisture"
Air temperature	**0.3029**	0.0786	−0.0746
Min air temperature	**0.3051**	0.0629	−0.0722
Max air temperature	**0.3009**	0.0909	−0.0775
Soil temperature (2 cm)	**0.3199**	−0.0431	−0.0522
Min soil temperature (2 cm)	**0.3189**	−0.0437	−0.0532
Max soil temperature (2 cm)	**0.3200**	−0.0425	−0.0514
Soil temperature (6 cm)	**0.3135**	−0.0669	−0.0400
Min soil temperature (6 cm)	**0.3134**	−0.0682	−0.0413
Max soil temperature (6 cm)	**0.3136**	−0.0659	−0.0388
RH	0.0550	**−0.4883**	−0.0383
Min RH	0.0550	**−0.4891**	−0.0344
Max RH	0.0512	**−0.4868**	−0.0361
PAR	−0.0251	−0.0876	**0.3839**
Min PAR	−0.0374	−0.0937	**0.4691**
Max PAR	0.0363	0.1655	**−0.3873**
VWC	−0.1787	−0.0820	**−0.3922**
Min VWC	−0.1772	−0.0893	**−0.3858**
Max VWC	−0.1703	−0.0700	**−0.3823**
VPD	0.1363	**0.4295**	−0.0050

Notes: PAR, photosynthetically active radiation; RH, relative humidity; VPD, vapor pressure deficit; VWC, volumetric water content. Values >0.25 (bold) were considered "heavily loading" on the axis.

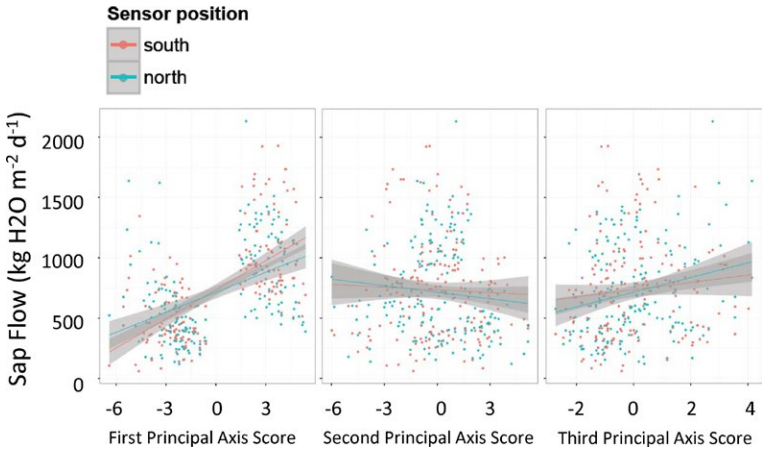


Fig. 1. Twenty-hour rates of sap flow across the growing season as a function of each of the first three principal axes. From left to right first principal score ranges from low to high temperature; second principal score ranges from low relative humidity (RH), high photosynthetically active radiation (PAR) and high vapor pressure deficit (VPD) to high RH, low PAR and low VPD; third principal score ranges from low to high soil moisture. Data are shown for the 12 experimental chambers.

only with soil moisture, and explained an additional 11.5% of the variance in the environmental variables for the daily sap flow data. A general linear model (GLM) of sensor position, the three principal components, and their interactions found a significant positive effect of *temperature* ($P < 0.0001$) and *soil moisture* ($P = 0.0001$) for daily sap flow rates, as well as an interaction between sensor position and *temperature* ($P = 0.02$; Table 5). The third axis of the nighttime data ("*PAR, soil moisture*") explained an additional 16.6% of the variance in environmental variables associated

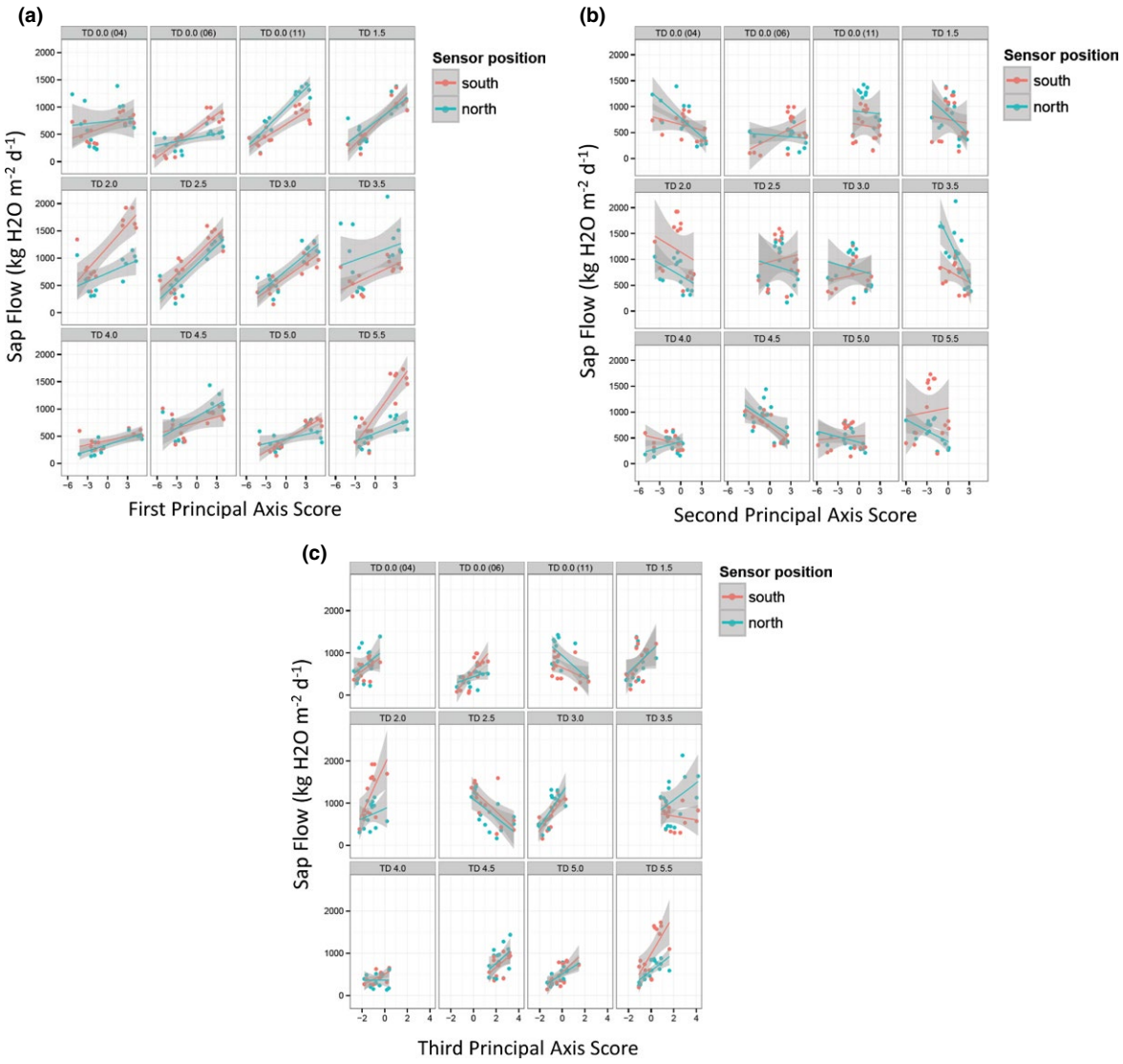


Fig. 2. (a) Twenty-hour rates of sap flow across the growing season and loadings as a function of first principal axis. From left to right first principal score ranges from low to high temperature. Data are shown for the 12 experimental chambers. (b) 24-h rates of sap flow across the growing season and loadings as a function of second principal axis. From left to right second principal score ranges from low relative humidity (RH), high photosynthetically active radiation (PAR) and high vapor pressure deficit (VPD) to high RH, low PAR and low VPD. Data are shown for the 12 experimental chambers. (c) 24-h rates of sap flow across the growing season and loadings as a function of third principal axis. From left to right third principal score ranges from low to high soil moisture. Data are shown for the 12 experimental chambers.

with nighttime sap flow and was positively correlated with average and minimum PAR, and negatively correlated with maximum PAR and all metrics of soil moisture. A GLM of sensor position, the three principal components, and their interactions confirmed that PC-3 (*PAR, soil moisture*) was significant ($P = 0.003$) and positively associated with nighttime sap flow (Table 6).

Last, HDD was included as an environmental variable along with the three PCA axes for the regression of early growing season sap flow both over the course of a 24-h day and for nighttime

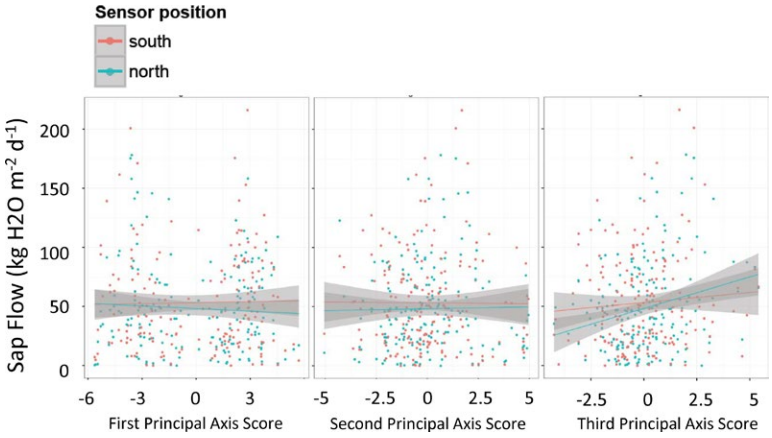


Fig. 3. Nighttime rates of sap flow throughout the growing season and loadings as a function of each of the first three principal axes. From left to right, first principal score ranges from low to high temperature; second principal score ranges from low relative humidity (RH), high photosynthetically active radiation (PAR) and high vapor pressure deficit (VPD) to high RH, low PAR and low VPD; third principal score ranges from low to high soil moisture. Data are shown for the 12 experimental chambers.

sap flow. Our GLM of the 24-h, early season sap flow data showed that PC-1 (*temperature)* was correlated significantly and positively with early growing season sap flow ($P < 0.0001$), and sensor position on the tree (i.e., south vs. north) was significant as well ($P = 0.012$, Table 7; Figs. 5 and 6). GLM of the nighttime early sap flow data (Table 8) showed HDD to be significantly positively correlated with nighttime sap flow ($P = 0.0053$). PC-1 ($P = 0.049$, *temperature*) and PC-3 ($P = 0.017$, *PAR*, *soil moisture*) both were correlated significantly and positively with nighttime sap flow in the early growing season.

Discussion

The objective of this study was to examine how projected warming in the northeastern United States may affect water uptake by trees; such effects could have important implications for hydrological budgets of forested ecosystems. Rates of sap flow measured in this study were within the range reported for other temperate deciduous forests (Bovard et al. 2005, Daley and Phillips 2006), and we found that warmer air and surface soil temperatures led to elevated rates of sap flow in mature red oak trees. Previous research has found air temperature, VPD, and PAR correlated most closely with rates of transpiration (Granier et al. 1996b, PengSen et al. 2000, Yin et al. 2004, Bovard et al. 2005, Juhász et al. 2013). Similarly, water uptake by roots has been found to increase with increasing temperatures up to 26°C (Lopushinsky and Kaufmann 1984). Delf (1916) found similar results up to 35°C, above which root permeability decreased, presumably due to cell injury. Soil temperatures in our study did not exceed 22°C, which is within the range of previously studied temperatures correlated with increased root uptake of water.

Our results agree with a previous soil warming study which found elevated spring time sap flow in Norway spruce trees experiencing elevated soil temperatures (Bergh and Linder 1999). Previous research also found colder soils to be associated with reduced water uptake by plants, largely due to increased viscosity of water as well as decreased root permeability (Kramer 1940, Lopushinsky and Kaufmann 1984). Within the natural range of variation, greater soil temperatures have been found to increase root growth (Tryon and Chapin 1983) and shoot growth (Weih and Karlsson 2001), as well as rates of nutrient uptake (Chapin 1974, Karlsson and Nordell 1996, Weih and Karlsson 1999, 2001). We found air and surface soil temperature to be the strongest predictor of sap flow rates both across the growing season and in the early growing season. Soil moisture also was found to be correlated positively with sap flow rates across the growing season, at night, and in the early growing season at night.

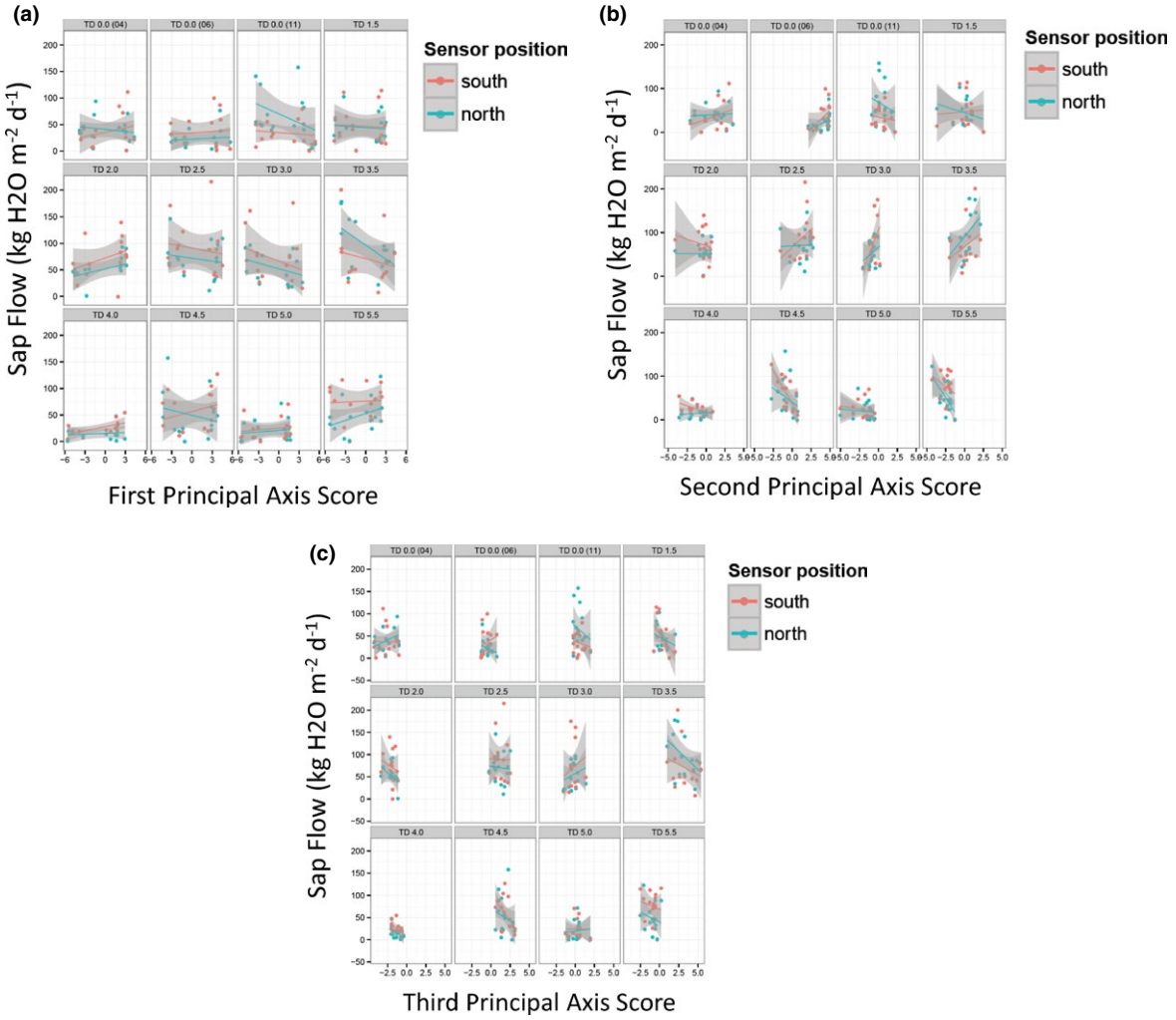


Fig. 4. (a) Nighttime rates of sap flow throughout growing season and loadings as a function of first principal axis. From left to right, first principal score ranges from low to high temperature. Data are shown for the 12 experimental chambers. (b) Nighttime rates of sap flow throughout growing season and loadings as a function of second principal axis. From left to right second principal score ranges from low relative humidity (RH), high photosynthetically active radiation (PAR) and high vapor pressure deficit (VPD) to high RH, low PAR and low VPD. Data are shown for the 12 experimental chambers. (c) Nighttime rates of sap flow throughout growing season and loadings as a function of third principal axis. From left to right, third principal score ranges from low to high soil moisture. Data are shown for the 12 experimental chambers.

Although it has often been assumed that transpiration ceases at night, mounting evidence demonstrates the continuation of transpiration during hours of darkness, and its importance for accurately estimating total ecosystem transpiration rates (Daley and Phillips 2006, Dawson et al. 2007, Fisher et al. 2007, Oishi et al. 2008, Phillips et al. 2010). Nighttime transpiration could be altered in the future as the global climate warms, as there have been many observations showing that nighttime temperatures are increasing faster than daytime temperatures (Alexander et al. 2006). Previous work at Harvard Forest also found nighttime sap flow in red oak trees to account for more than 8% of total daily sap flow, and to be partially associated with recharging water stores depleted during the day (Daley and Phillips 2006). Nocturnal sap flow also stops when daytime VPD is very high or

Table 5. Results of general linear model of 24-h sap flow as a function of sensor position, the three principal components, and their interactions.

	df	MS	*F*	*P*
Sensor	1	3.7×10^{10}	0.36	0.55
PC-1 (*temperature*)	1	1.6×10^{13}	156.84	**<0.0001**
PC-2 (*RH, PAR, VPD*)	1	2.9×10^{11}	2.78	0.10
PC-3 (*soil moisture*)	1	1.6×10^{12}	15.35	**0.0001**
Sensor × PC-1	1	5.5×10^{11}	5.30	**0.02**
Sensor × PC-2	1	5.0×10^{10}	0.48	0.49
Sensor × PC-3	1	1.8×10^{11}	1.73	0.19
Residuals	346	3.6×10^{13}		

Note: PAR, photosynthetically active radiation; RH, relative humidity; VPD, vapor pressure deficit. Bold p-values indicate statistical significance ($P<0.05$).

Table 6. Results of general linear model of nighttime sap flow as a function of sensor position, the three principal components, and their interactions.

	df	MS	*F*	*P*
Sensor	1	2.2×10^{9}	1.42	0.23
PC-1 (*temperature)*	1	1.7×10^{8}	0.11	0.74
PC-2 (*RH, VPD)*	1	9.1×10^{6}	0.01	0.94
PC-3 (*PAR, soil moisture)*	1	1.4×10^{10}	8.80	**0.003**
Sensor × PC-1	1	8.6×10^{8}	0.55	0.46
Sensor × PC-2	1	7.6×10^{7}	0.05	0.83
Sensor × PC-3	1	3.6×10^{9}	2.33	0.13
Residuals	346	1.6×10^{9}		

Note: PAR, photosynthetically active radiation; RH, relative humidity; VPD, vapor pressure deficit. Bold p-values indicate statistical significance ($P<0.05$).

Table 7. Results of general linear model of early growing season sap flow (24-h) as a function of sensor position, heating degree days (HDD), the three principal components, and their interactions.

	df	MS	*F*	*P*
Sensor	1	5.3×10^{11}	6.65	**0.0116**
HDD	1	1.6×10^{11}	2.04	0.16
PC-1 (*temperature)*	1	1.9×10^{12}	24.24	**<0.0001**
PC-2 (*RH, PAR, VPD)*	1	7.5×10^{10}	0.95	0.33
PC-3 (*soil moisture)*	1	4.7×10^{10}	0.59	0.44
Sensor × HDD	1	9.2×10^{9}	0.12	0.73
Sensor × PC-1	1	5.4×10^{10}	0.68	0.41
Sensor × PC-2	1	8.8×10^{9}	0.11	0.74
Sensor × PC-3	1	1.7×10^{9}	0.02	0.88
Residuals	86	7.9×10^{10}		

Note: PAR, photosynthetically active radiation; RH, relative humidity; VPD, vapor pressure deficit. Bold p-values indicate statistical significance ($P<0.05$).

soil moisture is very low (Daley and Phillips 2006, Dawson et al. 2007). These findings are consistent with our results; we found increased nocturnal sap flow in chambers with relatively higher levels of soil moisture. Although there is very little work examining the relationship between temperature and nocturnal sap flow, one previous study found that rates of nighttime sap flow in *Picea engelmanii* were lower in colder soils (Day et al. 1990). We did not observe a significant effect of temperature on

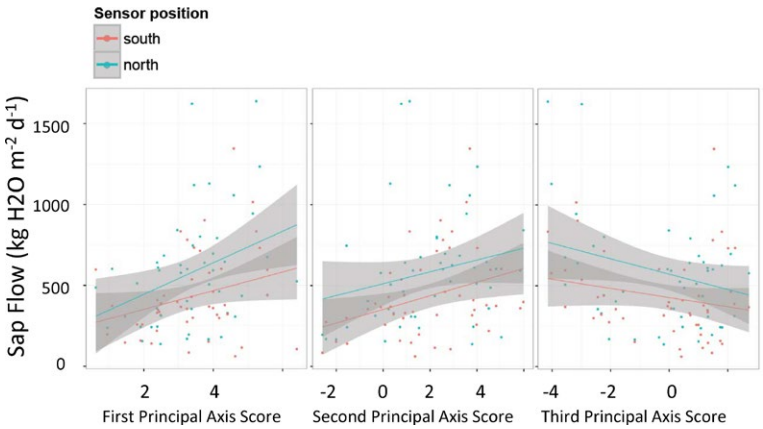


Fig. 5. Twenty-hour rates of sap flow in early growing season and as a function of the first three principal axes. From left to right, first principal score ranges from low to high temperature; second principal score ranges from low relative humidity (RH), high photosynthetically active radiation (PAR) and high vapor pressure deficit (VPD) to high RH, low PAR and low VPD; third principal score ranges from low to high soil moisture. Data are shown for the 12 experimental chambers.

rates of night time sap flow across the measurement period, but did observe a positive correlation between temperature and nighttime sap flow in the early growing season.

We found temperature to be the dominant driver of sap flow in the early growing season, both over the course of a 24-h day and at night. This result is consistent with previous studies, which found onset of photosynthesis in Korean pine trees to be triggered by increased springtime soil temperatures (Wu et al. 2013), and relatively later onset of photosynthesis in Scots pine trees due to delayed soil thawing (Strand et al. 2002). Similarly, in temperate deciduous forests, the onset of net C uptake in the early growing season has been predicted to occur when mean daily soil temperature equals mean annual air temperature (Baldocchi et al. 2005). Our warming treatments presumably warmed soil temperatures to the level of mean annual air temperature faster, and the trees therefore could have been phenologically advanced, resulting in greater rates of sap flow.

Winter temperatures also were found to have legacy effects on early growing season sap flow at night, with warmer winter temperatures leading to increased early season sap flow rates. This pattern could have resulted from reductions in soil freeze/thaw frequency. Warmer winter temperatures in our study reduced the number of soil freeze/thaw cycles, as well as the amount of time the soils spent below freezing (Fig. 7), which may have contributed to healthier roots with greater biomass at the beginning of the growing season. Soil freezing in winter has been shown to lead to frost heaving, which damages fine roots (Tierney et al. 2001, Comerford et al. 2013), impairing nutrient uptake by trees (Campbell et al. 2014). Warmer winter soils may therefore prevent root damage by preventing or diminishing soil freezing, leading to higher rates of water uptake in the early growing season. Elevated rates of sap flow in early spring due to warmer air and surface soil temperatures could result in an overall increase in tree water uptake and canopy gas exchange, with potential consequences for forest water dynamics.

Conclusions

As the climate changes, the growing season in the Northeast United States is getting warmer (Hayhoe et al. 2007), creating a longer period of activity for terrestrial vegetation (Schwartz et al. 2006, Polgar and Primack 2011). Given the large contribution of transpiration to total terrestrial water loss (Jasechko et al. 2013), the response of vegetation to changing climatic conditions will likely affect forest water budgets significantly. In our study, warmer air and soil temperatures led to elevated sap flow rates. However, warming also indirectly reduced rates of sap flow by decreasing soil moisture. The

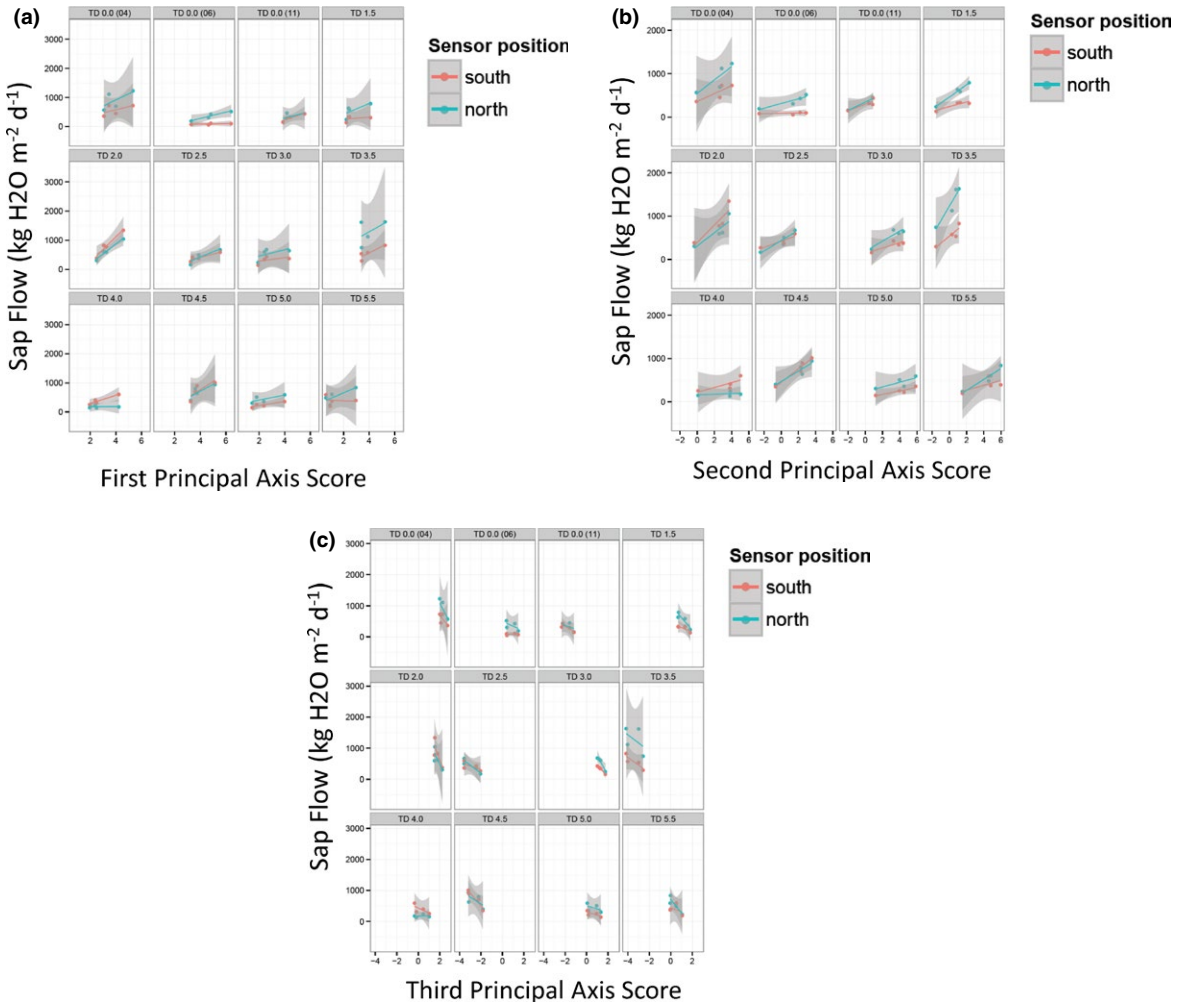


Fig. 6. (a) Twenty-hour rates of sap flow in early growing season as a function of the first principal axis. From left to right, first principal score ranges from low to high temperature. Data are shown for the 12 experimental chambers. (b) 24-h rates of sap flow in early growing season as a function of the second principal axis. From left to right, second principal score ranges from low relative humidity (RH), high photosynthetically active radiation (PAR) and high vapor pressure deficit (VPD) to high RH, low PAR and low VPD. Data are shown for the 12 experimental chambers. (c) 24-h rates of sap flow in early growing season as a function of the third principal axis. From left to right, third principal score ranges from low to high soil moisture. Data are shown for the 12 experimental chambers.

ultimate effect of warming on sap flow rates will therefore depend on both the direct effects of warming, and its indirect effects through alterations to soil moisture. We found the temperature increase to have a much greater effect on sap flow rates than did soil moisture levels. Because increased air temperatures are projected for this region, it is likely that rates of sap flow by red oak trees will increase in the future and forest trees may have higher water demand throughout the growing season. Hardwood forests in the northeastern United States have been considered a net carbon sink due to regeneration of forest ecosystems following agricultural abandonment in the 1850s (Turner et al. 1995, Fan et al. 1998, Houghton et al. 1999). Future carbon dynamics in these systems could change in response to projected changes

Table 8. Results of general linear model of nighttime early growing season sap flow as a function of sensor position, heating degree days (HDD), the three principal components, and their interactions.

	df	MS	*F*	*P*
Sensor	1	3.6×10^8	0.39	0.54
HDD	1	7.7×10^9	8.20	**0.00527**
PC-1 (*temperature)*	1	3.7×10^9	4.00	**0.04859**
PC-2 (*RH, VPD)*	1	1.0×10^8	0.11	0.74
PC-3 (*PAR, soil moisture)*	1	5.5×10^9	5.88	**0.01746**
Sensor × HDD	1	2.3×10^9	2.50	0.12
Sensor × PC-1	1	2.6×10^7	0.03	0.87
Sensor × PC-2	1	2.4×10^8	0.26	0.61
Sensor × PC-3	1	2.8×10^6	0.00	0.96
Residuals	86	9.3×10^8		

Note: PAR, photosynthetically active radiation; RH, relative humidity; VPD, vapor pressure deficit. Bold p-values indicate statistical significance ($P<0.05$).

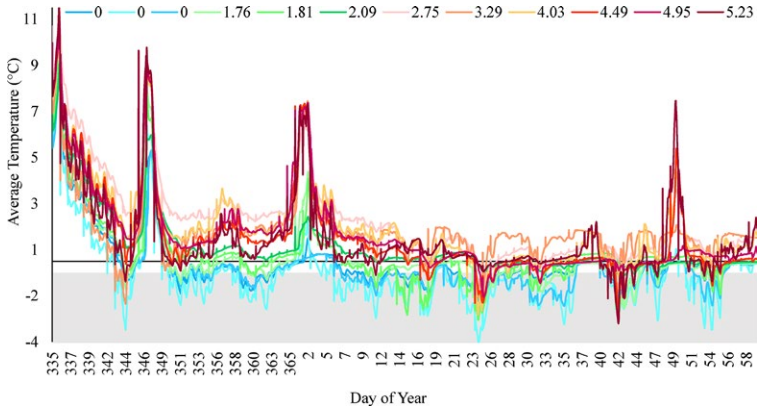


Fig. 7. Mean soil temperature at 2 cm depth measured in each chamber from 1 December 2010 to 28 February 2011 [days of year (DOY) 335–59]. Legend values are the average increase in air temperature ($\Delta T_{chamber}$) for each chamber during the sap flow measurement period. The shaded area denotes freezing soil temperatures between −0.5°C and −4°C. Fine roots experiencing the low end of this temperature range have been shown to experience elevated rates of mortality (Tierney et al. 2001).

in climate if the ability of trees to take up water is increased further. Our results suggest that under warming conditions, sap flow rates likely will increase with potential consequences for forest water availability and therefore productivity of vegetation.

Acknowledgments

We thank Christine Bollig for valuable assistance with field installation of sap flow sensors and Mark VanScoy and the staff of Harvard Forest for logistical support and assistance. Keita DeCarlo and Julianne Richard helped build sap flow sensors in the lab. Sap flow conversions were done using BaseLiner, which was developed by Ram Oren's C-H_2O Ecology Lab Group at the Nicholas School of the Environment at Duke University. Software development of BaseLiner was supported by the Biological and Environmental Research Program (BER), US Department of Energy through the Southeast Regional Center (SERC) of the National Institute for Global Environmental Change (NIGEC), and through the Terrestrial Carbon Process Program (TCP). The infrastructure development and operations of the chambers was supported by the US Department of Energy (grant DE-FG02-08ER64510) and the US NSF

Dimensions of Biodiversity Program (grant DEB 1136646). Research was supported by the Northeastern States Research Cooperative, a joint program of the University of Vermont, the University of Maine and the United States Department of Agriculture Forest Service, Northern Research Station. Grant No. 1149929 from the NSF DEB Program provided partial support to Templer during the writing of this paper.

AE conceived the warming experiment. PT, NP, and SJ conceived the project. SJ and SP performed research in the field; SJ, AE, and PT analyzed the data; SJ and PT wrote the manuscript; AE, NP, and SP contributed to editing of the manuscript.

Literature Cited

Alexander, L. V., et al. 2006. Global observed changes in daily climate extremes of temperature and precipitation. Journal of Geophysical Research: Atmospheres 111:1–22.

Baldocchi, D. D., et al. 2005. Predicting the onset of net carbon uptake by deciduous forests with soil temperature and climate data: a synthesis of FLUXNET data. International Journal of Biometeorology 49:377–387.

Bergh, J., and S. Linder. 1999. Effects of soil warming during spring on photosynthetic recovery in boreal Norway spruce stands. Global Change Biology 5:245–253.

Boose, E. 2001. Fisher Meteorological Station at Harvard Forest since 2001. Harvard Forest Data Archive: HF001.

Bovard, B. D., P. S. Curtis, C. S. Vogel, H. B. Su, and H. P. Schmid. 2005. Environmental controls on sap flow in a northern hardwood forest. Tree Physiology 25:31–38.

Campbell, J. L., A. M. Socci, and P. H. Templer. 2014. Increased nitrogen leaching following soil freezing is due to decreased root uptake in a northern hardwood forest. Global Change Biology 20:2663–2673.

Chang, X., W. Zhao, and Z. He. 2014. Radial pattern of sap flow and response to microclimate and soil moisture in Qinghai spruce (*Picea crassifolia*) in the upper Heihe River Basin of arid northwestern China. Agricultural and Forest Meteorology 187:14–21.

Chapin, F. S. 1974. Morphological and physiological mechanisms of temperature compensation in phosphate absorption along a latitudinal gradient. Ecology 55:1180–1198.

Clearwater, M. J., F. C. Meinzer, J. L. Andrade, G. Goldstein, and N. M. Holbrook. 1999. Potential errors in measurement of nonuniform sap flow using heat dissipation probes. Tree Physiology 19:681–687.

Comerford, D. P., P. G. Schaberg, P. H. Templer, A. M. Socci, J. L. Campbell, and K. F. Wallin. 2013. Influence of experimental snow removal on root and canopy physiology of sugar maple trees in a northern hardwood forest. Oecologia 171:261–269.

Cottingham, K. L., J. T. Lennon, and B. L. Brown. 2005. Knowing when to draw the line: designing more informative ecological experiments. Frontiers in Ecology and the Environment 3:145–152.

Daley, M. J., and N. G. Phillips. 2006. Interspecific variation in nighttime transpiration and stomatal conductance in a mixed New England deciduous forest. Tree Physiology 26:411–419.

Daley, M. J., N. G. Phillips, C. Pettijohn, and J. L. Hadley. 2007. Water use by eastern hemlock (*Tsuga canadensis*) and black birch (*Betula lenta*): implications of effects of the hemlock woolly adelgid. Canadian Journal of Forest Research 37:2031–2040.

Dawson, T. E., S. S. O. Burgess, K. P. Tu, R. S. Oliveira, L. S. Santiago, J. B. Fisher, K. A. Simonin, and A. R. Ambrose. 2007. Nighttime transpiration in woody plants from contrasting ecosystems. Tree Physiology 27:561–575.

Day, T. A., E. H. Delucia, and W. K. Smith. 1990. Effect of soil temperature on stem sap flow, shoot gas exchange and water potential of *Picea engelmanii* (Parry) during snowmelt. Oecologia 84:474–481.

Delf, E. M. 1916. Studies of protoplasmic permeability by measurement of rate of shrinkage of turgid tissues I. The influence of temperature on the permeability of protoplasm to water. Annals of Botany 2:283–310.

Fan, S., M. Gloor, J. Mahlman, S. Pacala, J. Sarmiento, T. Takahashi, and P. Tans. 1998. A large terrestrial carbon sink in North America implied by atmospheric and oceanic carbon dioxide data and models. Science 282:442–446.

Feng, S., and Q. Fu. 2013. Expansion of global drylands under a warming climate. Atmospheric Chemistry and Physics 13:10081–10094.

Fisher, J. B., D. D. Baldocchi, L. Misson, T. E. Dawson, and A. H. Goldstein. 2007. What the towers don't see at night: nocturnal sap flow in trees and shrubs at two AmeriFlux sites in California. Tree Physiology 27:597–610.

Ford, C. R., and J. M. Vose. 2007. *Tsuga canadensis* (L.) Carr. mortality will impact hydrologic processes in southern appalachian forest ecosystems. Ecological Applications 17:1156–1167.

Foster, D. R. 1992. Land-use history (1730–1990) and vegetation dynamics in central New England, USA. Ecology 80:753–771.

Foster, D. R., and J. D. Aber. 2004. Page# 496p Forests in time, the environmental consequences of

1,000 years of change in New England. Yale University Press, New Haven, Connecticut.

Granier, A. 1987. Evaluation of transpiration in a Douglas-fir stand by means of sap flow measurements. Tree Physiology 3:309–320.

Granier, A., T. Anfodillo, M. Sabatti, H. Cochard, E. Dreyer, M. Tomasi, R. Valentini, and N. Breda. 1994. Axial and radial water-flow in the trunks of oak trees: a quantitative and qualitative analysis. Tree Physiology 14:1383–1396.

Granier, A., P. Biron, N. Breda, J. Y. Pontailler, and B. Saugier. 1996a. Transpiration of trees and forest stands: short and longterm monitoring using sapflow methods. Global Change Biology 2:265–274.

Granier, A., R. Huc, and S. T. Barigah. 1996b. Transpiration of natural rain forest and its dependence on climatic factors. Agricultural and Forest Meteorology 78:19–29.

Hayhoe, K., et al. 2007. Past and future changes in climate and hydrological indicators in the US Northeast. Climate Dynamics 28:381–407.

Horton, R., G. Yohe, W. Easterling, R. Kates, M. Ruth, E. Sussman, A. Whelchel, D. Wolfe, and F. Lipschultz. 2014. Ch. 16: Northeast. In Climate Change Impacts in the United States: The Third National Climate Assessment. J. M. Melillo, T. C. Richmond, and G. W. Yohe, eds. U.S. global change research program, 371–395, doi:10.7930/J0SF2T3P. Washington, D.C.

Houghton, R. A., J. L. Hackler, and K. T. Lawrence. 1999. The US carbon budget: contributions from land-use change. Science 285:574–578.

James, S. A., M. J. Clearwater, F. C. Meinzer, and G. Goldstein. 2002. Heat dissipation sensors of variable length for the measurement of sap flow in trees with deep sapwood. Tree Physiology 22:277–283.

Jasechko, S., Z. D. Sharp, J. J. Gibson, S. J. Birks, Y. Yi, and P. J. Fawcett. 2013. Terrestrial water fluxes dominated by transpiration. Nature 496:347–350.

Juhász, Á., P. Sepsi, Z. Nagy, L. Tőkei, and K. Hrotkó. 2013. Water consumption of sweet cherry trees estimated by sap flow measurement. Scientia Horticulturae 164:41–49.

Karlsson, P. S., and K. O. Nordell. 1996. Effects of soil temperature on the nitrogen economy and growth of mountain birch seedlings near its presumed low temperature distribution limit. Ecoscience 3:183–189.

Kramer, P. J. 1940. Root resistance as a cause of decreased water absorption by plants at low temperatures. Plant Physiology 15:63.

Lopushinsky, W., and M. R. Kaufmann. 1984. Effects of cold soil on water relations and spring growth of douglas fir seedlings. Forest Science 30:628–634.

Lu, P., L. Urban, and P. Zhao. 2004. Granier's thermal dissipation probe (TDP) method for measuring sap flow in trees: theory and practice. Acta Botanica Sinica 46:631–646.

McFarlane, K. J., M. S. Torn, P. J. Hanson, R. C. Porras, C. W. Swanston, M. A. Callaham, and T. P. Guilderson. 2013. Comparison of soil organic matter dynamics at five temperate deciduous forests with physical fractionation and radiocarbon measurements. Biogeochemistry 112:457–476.

Oishi, A. C., R. Oren, and P. C. Stoy. 2008. Estimating components of forest evapotranspiration: a footprint approach for scaling sap flux measurements. Agricultural and Forest Meteorology 148:1719–1732.

Pelini, S. L., F. P. Bowles, A. M. Ellison, N. J. Gotelli, N. J. Sanders, and R. R. Dunn. 2011. Heating up the forest: open-top chamber warming manipulation of arthropod communities at Harvard and Duke Forests. Methods in Ecology and Evolution 2:534–540.

PengSen, S., M. LuYi, W. Xiaoping, and Z. MingPu. 2000. Temporal and spatial variation of sap flow of Chinese pine (*Pinus tabulaeformis*). Journal of Beijing Forestry University 22:1–6.

Phillips, N., R. Oren, and R. Zimmermann. 1996. Radial patterns of xylem sap flow in non-, diffuse- and ring-porous tree species. Plant, Cell & Environment 19:983–990.

Phillips, N., J. D. Lewis, B. A. Logan, and D. T. Tissue. 2010. Inter- and intra-specific variation in nocturnal water transport in Eucalyptus. Tree Physiology 30:586–596.

Polgar, C. A., and R. B. Primack. 2011. Leaf-out phenology of temperate woody plants: from trees to ecosystems. New Phytologist 191:926–941.

R Core Team. 2013. R: A language and environment for statistical computing. R Foundation for Statistical Computing, Vienna, Austria URL https://www.R-project.org/

Scheff, J., and D. M. W. Frierson. 2014. Scaling potential evapotranspiration with greenhouse warming. Journal of Climate 27:1539–1558.

Schwartz, M. D., R. Ahas, and A. Aasa. 2006. Onset of spring starting earlier across the Northern Hemisphere. Global Change Biology 12:343–351.

Strand, M., T. Lundmark, I. Söderbergh, and P.-E. Mellander. 2002. Impacts of seasonal air and soil temperatures on photosynthesis in Scots pine trees. Tree Physiology 22:839–847.

Swanson, R. H. 1994. Significant historical developments in thermal methods for measuring sap flow in trees. Agricultural and Forest Meteorology 72:113–132.

Tierney, G. L., T. J. Fahey, P. M. Groffman, J. P. Hardy, R. D. Fitzhugh, and C. T. Driscoll. 2001. Soil freezing alters fine root dynamics in a northern hardwood forest. Biogeochemistry 56:175–190.

Tryon, P. R., and F. S. Chapin. 1983. Temperature control over root growth and root biomass in taiga forest trees. Canadian Journal of Forest Research 13:827–833.

Turner, D. P., G. J. Koerper, M. E. Harmon, and J. J. Lee. 1995. A carbon budget for forests of the conterminous United States. Ecological Applications 5:421–436.

Weih, M., and P. S. Karlsson. 1999. The nitrogen economy of mountain birch seedlings: implications for winter survival. Journal of Ecology 87:211–219.

Weih, M., and P. S. Karlsson. 2001. Growth response of Mountain birch to air and soil temperature: is increasing leaf-nitrogen content an acclimation to lower air temperature? New Phytologist 150:147–155.

Wu, J. B., D. X. Guan, F. H. Yuan, A. Z. Wang, and C. J. Jin. 2013. Soil temperature triggers the onset of photosynthesis in Korean pine. PLoS ONE 8:e65401.

Yin, G. C., G. Y. Zhou, J. Morris, Z. H. Huang, G. W. Chu, and G. Y. Zhou. 2004. Sap flow response of *Eucayluptus urophylla* to environmental stress in south China. Journal of Zhejiang University Science 5:1218–1225.